Alexandria Journal of Science and Technology

Article

New green insight into sustainable Moringa oleifera : *in vitro* synergetic study with Cyclophosphamide S.

Samira A. Mosaad [1,*], Farozia I. Moussa [1], Horeya S. A. El Gawad [1], Salwa S. Mahmoud [1], Howida A. Fetouh [2,*]

[1] *Zoology Department, Faculty of Science, Alexandria University.*

[2] *Chemistry Department, Faculty of Science, Alexandria University.*

[*] *Correspondence Address:*

Samira A. Mosaad: Zoolgy Department, Faculty of Science, Alexandria University. Email address: SamiraAdeeb@alexu.edu.eg.

Howida A.Fetouh: Chemistry Department, Faculty of Science, Alexandria University. Email address: howida_fetouh@alexu.edu.eg.

KEYWORDS: Cyclophosphamide, Ultra sound, heat, extraction, cancer.

Received:
July 16, 2024

Accepted:
November 08, 2024

Published:
December 16, 2024

ABSTRACT: To achieve the aim of the present study as evaluation of the medicinal moringa oleifera leaf extract (MOLE) in combination of antitumor cyclophosphamide to replace the effective steroidal drugs that have many side effects such as obesity, high blood pressure and depression. New extraction method using ultrasonic radiation in water green solvent was employed. Ultrasonic assisted extraction yielded more bioactive compounds as compared to conventional heat extraction. Comparative FTIR spectra, impedance, cyclic voltammetry and chromatography confirmed validation of ultrasound extraction improving yield and quality in addition to heat energy and time spacing. The extraction time and frequency of ultrasound radiation qualitatively and quantitatively affect quality and concentration of extracted phytochemicals. The aqueous ultrasound MOLE showed synergism with Cyclophosphamide (CPA) as potent antioxidant and antitumor agent to breast cancer. The MOLE extracts mitigated toxicity of CPA by decreasing the values of the fifty inhibitory concentrations (IC_{50}) from 198.88 µg/mL to 95.2 µg/mL. This finding suggested *in vivo* and clinical trials for using USMOLE-CPA combination therapy.

1. INTRODCTION

Cyclophosphamide (CPA) is active anticancer drug for treatment different types of multiple human malignancies and disorders [1]; immunosuppressive agent used in combination chemotherapy for Hodgkin lymphoma (HL) and non-Hodgkin lymphoma, breast, endometrial and lung cancer, leukemia, burrkitts lymphoma, lupus erythematosus, rheumatoid arthritis, multiple (sclerosis, myeloma, neuroplastoma [2]. CPA-based regimens included: total body irradiation (TBI) then high dose; Fludarabine-CPA less toxic and effective in some patients; busulfan-CPA used if TBI-CPA intolerant. Both TBI-CPA and FluCPA regimens prevent GVHD in HLA-matched donor transplants in HL; reduced dose TBI-CPA reduce GVHD risk and complications. Haploidentical donor transplants increased GVHD risk more than HLA-matched transplants. CPA regimens used but was not optimized. The GVHD risk could be reduced by *in vivo* depletion of donor T cells or post-CPA transplant. CPA regimens prevent GVHD in both HLA-matched and haploidentical donor transplants for HL patients. Regimen and additional strategies selected based on the patient's age, disease stage and donor availability [2].

CPA clinically restricted by multiple side effects [3]. Bio activation generates reactive oxygen species (ROS) oxidative damage and modified components of both neoplastic and normal cells [4]. Alkylating agent N-mustard contains electrophilic alkyl group (R) attacks nucleophilic moieties of DNA or proteins causing covalent transfer of R group [5]. The metabolites acrolein and phosphoramidemustard (exerts antineoplastic effects *via* irreversible cross-linking DNA strands at N-7guanine position (**Figure 1**) causing cell death [6]. A single large dose caused: hemorrhagic cell death and heart failure [7]. N-mustard transformed into aziridinium ion interacts with another DNA nucleophile caused DNA crosslinking [5]. CPA activated by CYP450 enzyme giving unstable precursors freely diffuse into cancer cells 4-OH-CPA tautomer form phosphamide that decomposed *via* β-elimination reaction giving acrolein byproduct and active cytotoxic phosphoramide mustard forming both inter- and intra-strand DNA crosslinking. Diffusion of the two non-cytotoxic intermediate metabolites depend on the cell type [8].

Alexandria Journal of Science and Technology, 2025, **3**(1), 01–10
Online ISSN: 2974-3273
DOI: 10.21608/ajst.2024.304865.1041

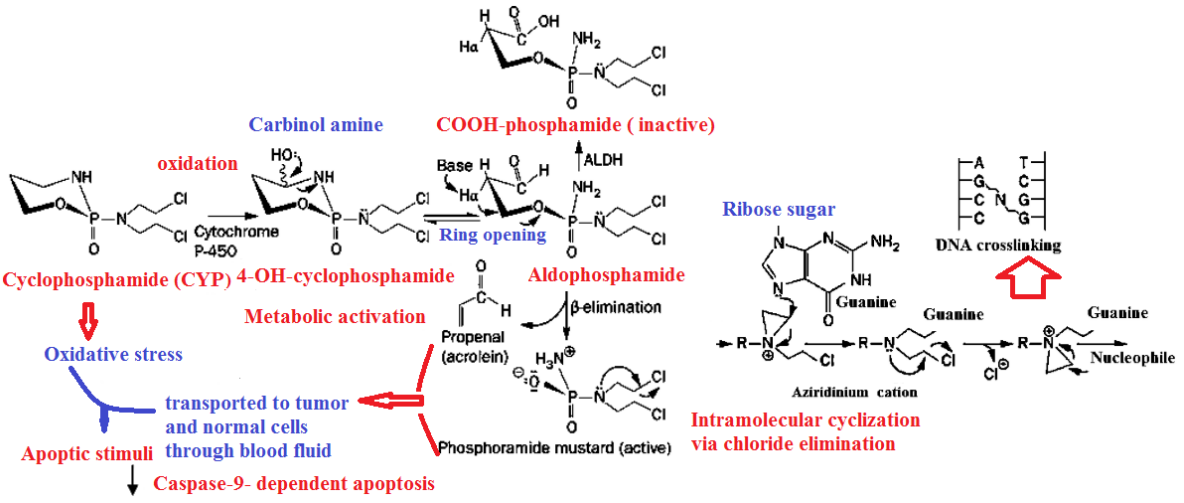

Figure 1. Major metabolic pathway of CPA inert prodrug enzymatically and chemically activated.

CHO-phosphamide oxidized into inactive metabolite COOH-CPA in hematopoietic stem cells *via* large amount expression aldehyde dehydrogenase [8]. Toxic acrolein increased ROS and lipid peroxidation hemorrhagic cystitis, bone marrow suppression, cardio-, gonadal toxicity and carcinogenesis on long uptake [9]. N-mustard cytotoxicity caused by reactive 2-Cl-ethyl groups. In physiological fluids, Cl^- ions eliminated from N mustards giving three membered cyclic aziridinium reactive cation linked DNA guanine bases [10]. N atom of alkylating agent releases and react with 2-Cl-ethyl side chain, forming second covalent linkage with another nucleophile (impact DNA replication by forming intrastrand DNA crosslinking) [10].

CPA induced cardio toxicity and failure by increasing ROS and reactive nitrogen species (RNS); react with protein caused cardiomyocyte swelling and inflammation, inhibited ATP production by altering mitochondrial calcium (Ca) overload, programmed cell death, nuclear splitting, vacuolization and signaling pathways [11]. Mitochondrial dysfunction and inflammation damage organs and reduced overall life quality. Oxidative stress by ROS oxidative damage mitochondria components. The subsequent production of ATPs energy units impaired causing cellular dysfunction and death. Disrupt Ca homeostasis in mitochondria causing further dysfunction and cell death. The chronic inflammation stimulated by the released pro-inflammatory cytokines and chemokines. Inflammatory mediators attract immune cells to the injury site and enhanced tissue damage. Antioxidant epoxylipids polyunsaturated fatty acids derivatives regulate inflammatory, protect mitochondria from oxidative damage.

CPA is immunosuppressive and antineoplastic drug but significantly causing thrombotic complications such as deep vein thrombosis (DVT), pulmonary embolism by activated platelets and disrupted coagulation pathways. CYP450 enzyme controlled CPA metabolism and toxicity, CPA exert directly affects thrombogenic endothelial cells even without CYP450 activation by enhancing platelets adhesion to endothelial surface, promoting aggregation and influence expression of adhesion molecules such as P-selectin and vascular cell adhesion molecule-1 which facilitate platelet and leukocyte adhesion, impair integrity and permeablilty of endothelial barrier, so pro-thrombotic factors released into blood stream, influence expression or activity of coagulation factors such as tissue factor and von Willebrand factor which contributing thrombus formation. ROS damage endothelial cells and promote pro-thrombotic responses, trigger inflammation cells and increased expression of pro-thrombotic factors and adhesion molecules, induce endoplasmic reticulum stress which contribute to cellular dysfunction and release pro-thrombotic factors.

MOLE mitigated CPA side effects such as nephro, hepato, cardio&immune toxicity and mutagenicity by high content of beta-carotene, minerals, Ca and K [12]. Anti-oxidants glycosylates, flavonoids, thiocarbamates and isothiocyanates scavenged ROS. Aqueous extract is potent free radical scavenger [13]. Antioxidant kaempferol is abundant [14]. Piperine and curcumin synergistically scavenged ROS induced by beryllium toxicity *in vivo* [15]. Alcoholic extract reduced glucose-induced cataractogenesis in isolated goat eye lenses by controlling of glautathion hormone (GSH) [16, 17].

Phytochemicals are more potent antioxidants than many chemicals such as isoquercetin, astragalin and crypto-chlorogenic [18]: Decreased levels of plasma monoaldehyde in fasting plasma glucose in healthy volunteers versus warm water control [19]. Safe dose alcoholic extract 100 $mgkg^{-1}$increased GSH and reduced levels monoaldehyde. Little single and solvents mixed examined include H_2O, acetone, CH_3OH, C_2H_5OH [20]. All reported *in vivo* studies used MOLE by conventional heat extraction [21] reported little chemicals in both aqueous and ethanolic extract. However, extraction of insoluble compounds required (acid/ alkali/enzymatic) [21].

In slow soxhlet extraction of powder plant, fresh water achieved complete extraction. Large amount water lost and some volatiles degraded at high temperature [22]. All reported extraction methods of MOLE have not optimized the extraction time,

temperature, solvent to sample ratio, number of extractions and particle size) although these parameters qualitatively and quantitatively control extraction yield and solubility of phytochemicals [21].

Steroidal drugs combined in chemotherapy by CPA effective in certain types of cancer, especially those involving inflammation or immunity dysfunction, suppressing the body's immune response to retard growth of cancer cells. However, these drugs showed health problems such as weight gain, high blood pressure and mood changes. Non-steroidal drugs are safe drugs and can be antitumor blocking production of certain enzymes causing inflammation and growth of cancer cell. However, non-steroidal drugs may be less effective in all cases. So this study aims achieving efficient green method for extraction method for MOL that be further evaluated in mitigation CPA cardio toxicity.

2. Experimental Design

2.1. Extraction of Moringa leaves

Aqueous MO leaves extract (MOLE) was obtained as: leaves collection, dried (de-humidification) at 35-40°C by a stream of hot air, grinded (decreasing size and homogenization) into fine powder. Conventional heat extract was done in comparison to Ultrasound irradiation (US) extraction (safe, rapid) [23] using Q700 sonicator/US homogenizer&emulsifier. A weight 5.0 g fine powder MOLE sonnicated in 50 mL double distilled water and extraction conducted at different frequencies 8 kHz, 16 kHz and 20 kHz for different times [23]. After extraction period, 10 mL suspension was placed in 25 mL capacity clean dry cold weighed beaker, after evaporation on hot plate, the calculated ppm concentration of hot extract was found 1728 ppm. Serial dilutions were carried out according to assay method. During experimental period, MOLE was kept in refrigerator in dark bottle to avoid photo degradation.

2.2. Characterization of Moringa leaves extract

FTIR (KBr) spectra of heat and US were recorded using Perkin Elmer spectrophotometer, 1430 at wavenumber range cm^{-1} (200-4000), polystyrene film calibration ($1602\pm1cm^{-1}$) [24]. Electrochemical behavior using cyclic voltammetry (CV) and impedance measurement in 3-electrode cell using: silver/silver chloride reference electrode (RE), Pt. wire counter electrode (CE) and graphite working electrode (WE) activated by alumina-double distilled water paste, 25 mL test MOLE solution. Cell was connected to Gamry potentiostate 600. After attaining rest potential of WE, impedance and CV recorded. Impedance of WE recorded by applying AC signal amplitude 10.0 mV at frequency range: 1 Hz to 100 kHz at rest potential [24]. 50 µL of 100 ppm MOLE distributed, air dried to 6 h at room temperature. 25 mL supporting electrolyte 0.1M $NaClO_4$ (increase electrical conductivity (CV were conducted at potential window 1.2 to -0.8 V, scene rate 0.01 Vs^{-1}. Data analyzed using E chem-analyst V 6.20 software program [25].

Gas chromatography-mass spectrometry (GC-MS) carried using Shimadzu Japan GC QP2010PLUS: fused column 2010 coated with poly-CH_3-silicon (0.25 nm diameter × 50 m length) at temperature range 80ºC to 200ºC): held 80º C, 1 min., rate 5°C min^{-1} and at 200°C for 20 min, field ionization detector at 300°C, injection temperature 220°C, nitrogen flow rate 1.0 mL min^{-1}, split ratio 1:75. Mobile phase flow rate 50 mL min^{-1}. The elute was emptied into a mass spectrometer with a detector voltage 1.5 kV and sampling rate 0.2 sec. connected to computerized mass spectra (MS) data bank, Hermlez 233 M-Z centrifuge (Germany). Phytochemicals were identified by comparison retention times (RT), peak area percentage and MS of fragmented ions with database in National Institute Standards Technology (NIST) digital library. Assay and purification by liquid chromatography with chemiluminescence based on chemical derivatization. Thermally stable MOLE analyzed using Gas Liquid Chromatography [26].

HPLC: stationary phase is Column C_8, UV-Vis. detector. Mobile phase: analytical grade 30% MeOH: 70% of (1%) acetic acid volume by volum mixture at flow rate 1.0 $mLmin.^{-1}$, filtered using micro filter paper 0.45 µm pore size and degassed in US waterbath [27]. Validation confirmed by constructing standard calibrated curve for series standard concentrations range (10 ppm - 50 ppm). Linearity evaluated by the linear least-squares regression method by weighting factor statistical analysis using micro cal. origin 20.0. Column efficiency determined from analyte peak equals or larger than 2000 theoretical plates. The peak tailing factor limited to 2.0. Relative standard deviation (RSD for injection replicates limited to 2.0%. Equal volumes 50 µL standard solution injected and chromatograms recorded with the major peaks responses. Limit of detection (LOD) and Limit of Quantitation (LOQ) calculated in ppm concentration. International Conference on Harmonization of Technical Requirements for Registration of Pharmaceuticals for Human use guidelines of validation analytical methods followed. The significance level at 5% confidence was used for evaluation. [27].

2.3. Evolution of some biological activity of Moringa leaves extract

Antibacterial activity of MOLE accessed by viable cell count colony-Forming Unit (CFU) P. aeruginosa local strain were inoculated directly into Lauryl sulfate (LS) broth culture medium: Tryptose for growth and nutrient source of N, C, SO_4^{-2} and trace ingredients; The fermentable Lactose sugar; LS inhibited organisms other than coliforms; K_3PO_4 buffer and NaCl for osmotic equilibrium. The culture media (recommended by American Public Health Association and the ISO Committee for coliforms detection). A weight 35.6 g LS Broth dispersion in 1000 mL double distilled water; placed into tubes containing inverted Durham's tubes; sterilization autoclaving at 15 lbs. pressure, 121°C for 15 min. The media used immediately after preparation, otherwise stored at 4°C until use. The remaining dry media stored at 24 °C. The enrichment media recovering the desired organisms. The presence of P. aeruginosa in the enrichment cultures became obvious via turbidity indicating active growth and fluorescence. After enrichment, bacteria were plated on solid LB media and purified using streaking plate method.

Antioxidant activities assayed using the stable free radical 1,1-diphenyl-2-picrylhydrazyl (DPPH•) versus ascorbic acid standard. 250 µL sample solution (50 mg dissolved in 1 mL DMSO) solvent added to 1 mL sample (6 mg/50 mL) DPPH/ DMSO solution. Sample volume completed to 3 mL with DMSO. The control was 3 mL DMSO. After Vortex mixture, incubation 30 min. in dark at room temperature the absorbance was measured at 517 nm [28].

The antitumor activity examined at Regional Center for Mycology and Biotechnology. In-vitro cytotoxicity of CPA and MO@CPA samples investigated using MTT assay in triplicates [29]. The tested human cancer cell lines were MCF-7 breast and normal lung cells MCR-5. Ninety six wells plates tissue culture plate inoculated with $1x10^5$ cells mL^{-1} according to American type culture collection: (100µL/well), incubation at physiological temperature 37°C for 24 h till. Monolayer confluent cells sheet formed. Growth medium decanted and cells washed twice with phosphate buffer solution. Two folds dilutions of test sample were prepared in maintenance RPMI medium with 2% serum. 0.1 mL dilution was tested in different wells leaving 3 wells as control receiving only maintenance medium and incubated at 37°C before examination. Physical signs of cells toxicity such as partial or loss monolayer, rounding, shrinkage or granulation monitored. 20 µL MTT solution (5 mg/mL in PBS) (BIO BASIC CANADA INC) added to wells, shacked for 5 min. at150 rpm, incubation (37ºC, 5% CO_2) for 2 h giving formazan crystals dissolved in 200 µL DMSO. Optical density (O.D.) of samples measured at λ560 nm. IC_{50} calculate the sigmoidal nonlinear fit of cell viability-concentration plot using origin 8.0 Lab. Northampton, NA) using equation 1.

$$\%\ cell\ viability = \frac{Absorbance\ _{test\ sample}}{Absorbance_{control}} \quad (1)$$

Where $A_{control}$ unreacted cell incubated with medium only assumed exhibited 100% cell viability.

3. Results and discussion

3.1. Characterization of MOLE

Figure 2 showed that US extraction yielded more bioactive volatile compounds in MOLE than heat extract. IR spectra bands showed ν (COOH) band at (1730-1732 cm^{-1}) range that was absent in heat extract. υ(NH) and δ(OH) were characteristics of heat MOLE. The US extract showed more functional groups at 1600cm^{-1}-500 cm^{-1} reflected many organic phytochemicals [28].

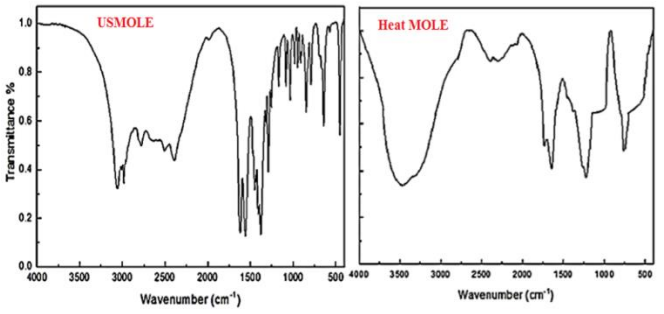

Figure 2. Comparative FTIR spectra of MOLE by US and heat extraction.

US extraction improved biochemical quality and yield. Conventional heat extraction less effective for the same MO powder-H_2O as water vapor penetrated the plant cells made loss of the most of volatile compounds [29].

The presence of more reactive organic in US extract was confirmed by Nyquist impedance plots in Figure 3 showed as the sized of the capacitive semicircles semicircle of USMOLE is larger than heat MOLE indicating more organic compounds adsorbed on the electrode surface [25].

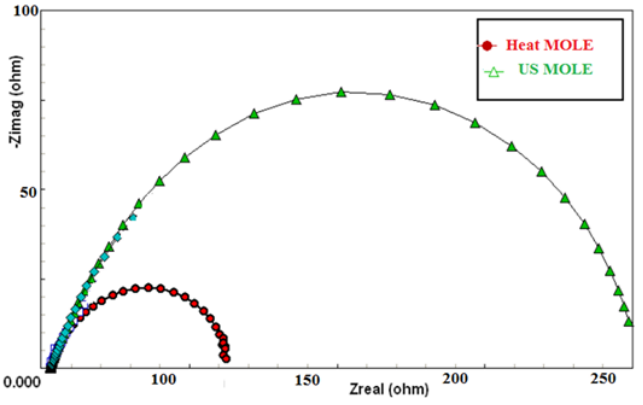

Figure 3. Comparative impedance plots of MOLEs.

The larger charge transfer (260 Ohm cm^{-1}) resistance equals semicircle diameter of US MOLE than heat extract (125 Ohm cm^{-1}) indicated the more adsorbed extracted adsorbed and impeded the passage of current [25]. CV plots, (Figure 4) confirmed the high concentration and larger mass transfer coefficient of ultrasound extract of moringa oleifera leaves (USMOLE) than the corresponding heat extract (heat MOLE).

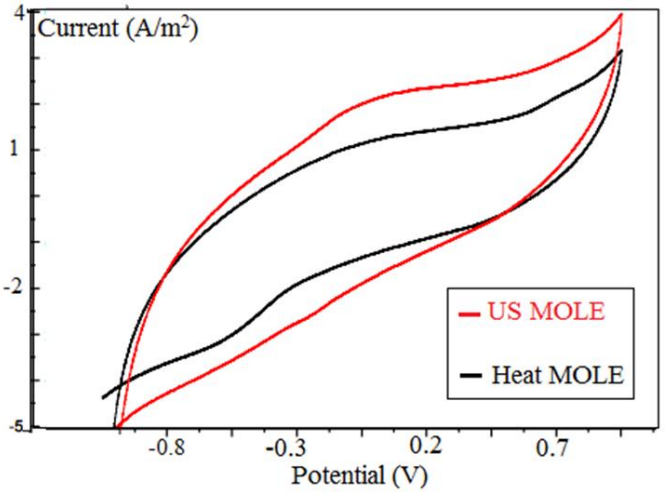

Figure 4. Comparative cyclic voltammograms of USMOLE and heat extract.

USMOLE (IPa/IPc (0.90), $k_{mass\ transfer}$ 16.1 cm/s) and heat extract ((IPa/IPc (0.081), $k_{mass\ transfer}$ 7.1 cm/s. The larger peak to peak current in USMOLE confirmed more extracted organic compounds [25].

Figure 5 showed GCMS chromatograms: Many peaks shown by USMOLE indicated more bioactive phytochemicals identified than heat extract [26].

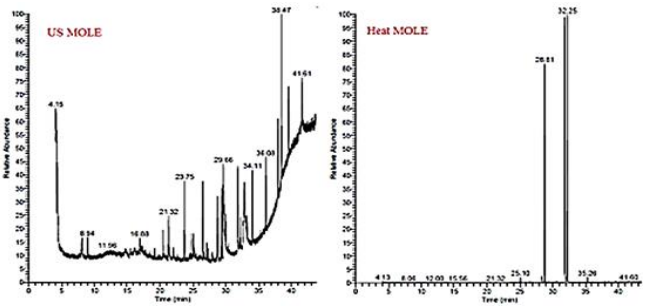

Figure 5. GCMS chromatograms of MOLE.

Safe and rapid ultrasound irradiation collapsing water bubbles generates a localized hot spots overheating heating and pressure 5000ºK and 20MPa respectively [30]. Few examples of antioxidants bioactive chemicals obtained from GCMS of USMOLE at retention time (Rt) were represented in Table 1.

Table 1: Some antioxidants phytochemicals from USMOLE

Compound name	Rt (min.)	Area %	Mw. (g/mol)	Molecular formula
Dodecanoic acid methyl ester	21.32	2.63	214	$C_{13}H_{26}O_2$
Pentadecanoic acid, 14-CH_3 ester	28.79	3.38	270	$C_{17}H_{34}O_2$
Di-n-octyl phthalate	38.47	8.82	390	$C_{24}H_{38}O_4$

Figure 6 showed the chemical structure of these phytochemicals showed similarity to ascorbic acid in some conjugation and carbonyl (C=O) group [31].

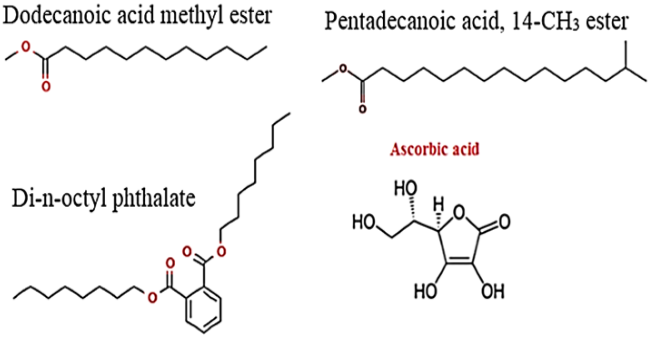

Figure 6. Chemical structure of MO antioxidant and ascorbic acid.

Although these phytochemicals similar to melatonin (**Figure 7**), neuro hormone synthesized and mainly secreted from mammalian pineal gland and other organs such as retina, extraorbital lacrimal gland, harderian gland, gastrointestinal tract, bone marrow cells and blood platelets.

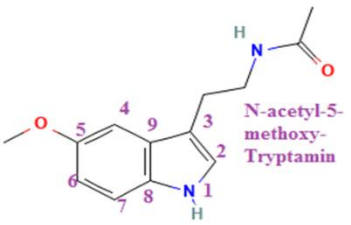

Figure 7. Molecular structure of the antioxidant melatonin.

It is non-enzymatic endogenous antioxidant prevents oxidation of other chemicals, protect cell components by neutralizing excess reactive free radicals which are natural byproducts of cell metabolism and produced by CPA and retard lipid oxidation.

Based on retention time (Rt), polarity of these compounds followed the order:

Di-n-octyl phthalate > Pentadecanoic acid, 14-CH ester > Dodecanoic acid methyl ester.

The less polar dodecanoic acid methyl ester take the longest Rt 38.47 min. to pass through silica stationary phase and detected. Water solubility of phytochemicals depends on intermolecular hydrogen bond (H.B.) with water molecules and ionization (ion-dipole intermolecular forces with water molecules). Solubility in water was predicted by applying empirical Lemke approach based on C-solubilizing potential of organic functional groups less than total No. of C atoms, compound is water-soluble 33]. Lipid solubility or lipophilicity due to large partition coefficient (P) between two immiscible liquid water and organic solvent such as chloroform [33].

$$\log P = \log(\frac{C_{organic}}{C_{aqueous}}) \quad (2)$$

Compound showed log P more than two are lipophilic rapidly penetrates CNS, less water soluble and not suitable for oral administration [33]. For these antioxidants phytochemicals target the site of action *via* interaction with: a lipophilic cell membrane and an aqueous cell cytoplasm and extracellular fluids and binding sites [34]. Hydrophilic lipophilic characteristics satisfied the conditions: polar (soluble in aqueous solution), polar/fatty interact with binding sites, sufficient lipophilic to across cell membrane and avoid rapid excretion. Very polar drug administrated by injection and is useful in gut infection [34].

The chromatogram of the mobile phase exhibited a peak at a retention time (RT) of 1.8 min. The peaks observed between 7.0 and 8.0 min. correspond to the bioactive compounds of MOLE. **Figure 8** displays the HPLC analysis of heat-treated MOLE, where weak, undefined peaks were detected within the RT range of 7.0 to 8.0 min. [25, 27].

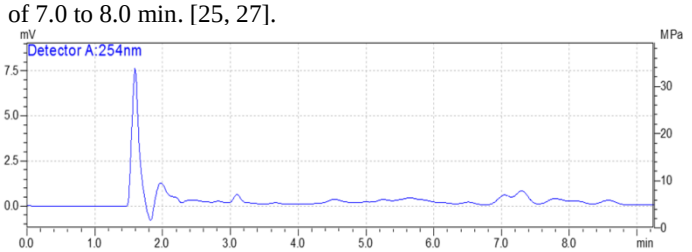

Figure 8. HPLC for heat MOLE.

For heat MOLE, weak peaks detected between Rt 7.0 min. to 8.0 min. **Figures 9-11** showed US HPLC at different frequencies.

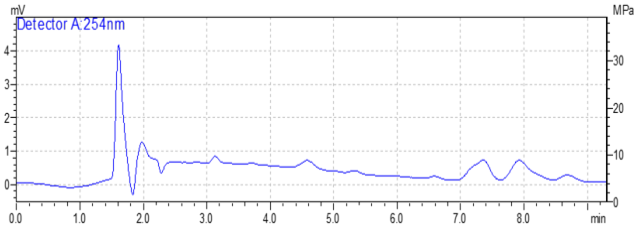

Figure 9. HPLC for US MOLE extracted at 8 kHz.

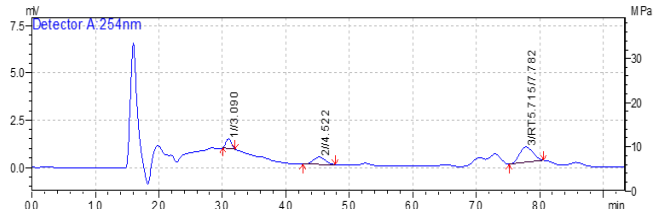

Figure 10. HPLC for US MOLE at 16 kHz.

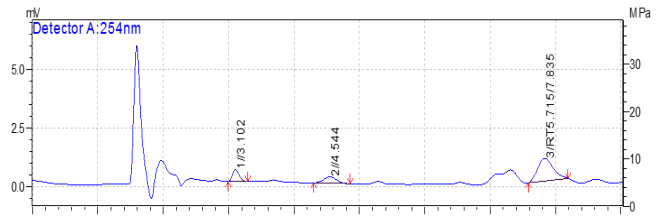

Figure 11. HPLC for US MOLE at 20 kHz.

Figure 12: confirmed validation of HPLC for quantification of MOLE [34].

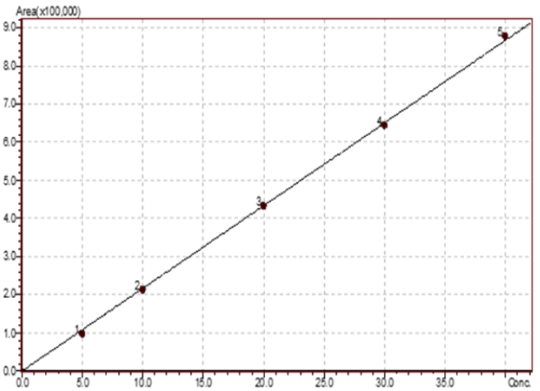

Figure 12. Standard calibration curve for HPLC.

Linear fitting of area under peak to concentration satisfied the regression equation

$y = ax + b = 21686.65\ x$ (correlation coefficient (R^2) was 0.9997 (3)

Figure 13 showed the area under peak and the corresponding concentration of MOLE. The ultrasound extract showed more wider area under peaks than the heat extract due to the larger numbers of phytochemicals in the former extract than the latter extract.

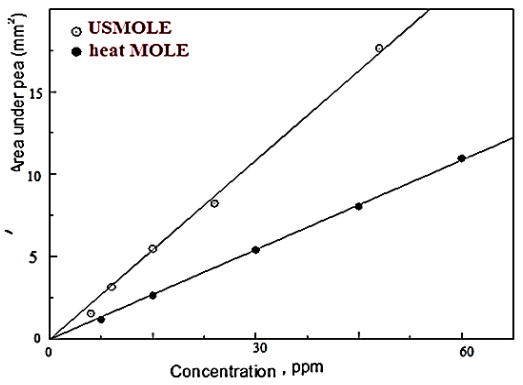

Figure 13. Variation of area under peak with concentration for MOLE

The limits of detection and quantification (LOD) and (LOQ) from HPLC were collected in Table 2.

Table 2: Detection limits of MOLE by HPLC [35].

MOLE	Standard deviation (σ)	Slope (S)	R^2	LOD x 10^3	LOQ
US	0.3118	0.4332	0.99901	2.235	7.45
Heat	0.0885	0.2169	0.99987	1.2348	4.1283

The low values LOD ($\frac{3\sigma}{S}$), and LOQ ($\frac{10\sigma}{S}$) (indicated the larger concentration of biochemical in USMOLE. than heat extract [35].

For USMOLE, area under peak (concentration) increased with extraction time and decreased with increasing frequency of radiation [36], **Figure 14**.

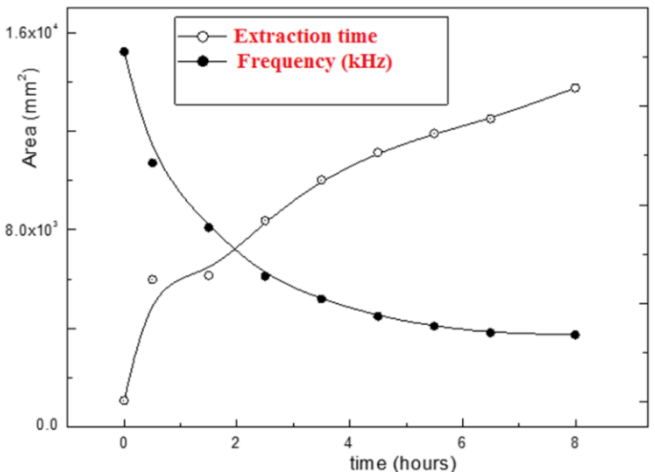

Figure 14. Effect of extraction time and frequency of US radiation on concentration of MOLE.

Rapid ultrasound (US) radiation: frequency (8Hz-100 kHz) propagate into MOL-H_2O mixture creating expansion and

compression cycles depending on frequencies. During rarefaction, small vacuum bubbles or voids nucleated and grow in water. Aggressive bubbles collapse at point when no longer energy absorbance during compression producing overheating and pressure up to 2000 atmosphere and 5000K disrupting plant cell walls. Cavitation released phytochemicals. H_2O penetrated channels produced by collapsed bubbles that increased permeability of cell wall membranes**.** US extraction was ten folds more efficient than hot water extraction for 12 h for same MOL- water mixture. The US wave dissolved cell contents by the homogeneous applied power. The bioactive chemicals diffused into water under concentration gradient and osmotic pressure. Low frequencies 20 kHz effectively extracted biochemical *via* cavitation. Bubbles at low frequencies are larger than those at high frequencies (20 kHz) implode violently and more effective extraction. Cavitation influenced by US intensity, gases, particle size, viscosity and surface tension. Optimization these factors increased will extraction yield [36].

3.2. Biological activity of MOLE

Figure 15 showed that US MOLE inhibited cell growth and proliferation and decreased colony formed viable cells.

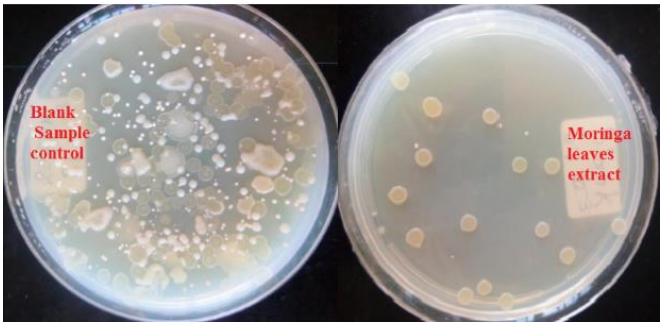

Figure 15. Visual inspection of CFU of MOLE.

MOLE kill bacteria and CFU become undetected after the microscopic count 3.0 x 10^6 cell mL^{-1}.

Anti-inflammatory bioactive phytochemicals of MOLE inhibited IκBα phosphorylation (protein binds to and reduce NFκB activation transcription factor that released and translocate to nucleus). The phosphorylated IκBα degraded. Blocking NFκB activation reduces expression of inflammatory proteins such as TNF-α, COX-2, IL-6, and iNOS. Reduced inflammation associated with obesity and contribute to metabolic disorders. Anti-inflammation alleviate arthriti symptoms such as joint pain and swelling. Treats type 2 diabetes and improve glycemic control, protected gastrointestinal mucosa to prevent or treat ulcers.

Table 3 showed antioxidants the most polar compounds of MOLE scavenged DPPH• by proton or electron transfer and inhibited DPPH reductase activity [37].

MOLE antioxidant scavenged DPPH• radical fairly good but less efficient than ascorbic acid; decreased oxidative stress and increased level of glutathione natural antioxidanr, improved CPA metabolism improved expression of hepatic CYP450 (1A2, 2C8/10, 2E1, 3A) proteins. Serum bilirubin independent on CYP content. Elevated serum bilirubin associated with significant declines in contents of CYP (1A2, 2C8/10) but not CYP (3A or 2E1). Nutritional MO affect concentration of serum bilirubin on levels CYP enzymes proteins mediated by cytokines, dietary composition and altered serum bile acids. Hence MOLE affect CYP expression and improved hepatic functions [38]. Specific CYPs in various tissues, especially liver controlled CPA metabolism, catalyze redox metabolic reactions and ester or amides hydrolysis and facilitate clearance of water-soluble metabolites through kidneys or bile. In some cases, CPA metabolism gave toxic metabolites cause liver damage or allergy. CYPs can enhance CPA interaction with another drug metabolized by same the CYP.

Because the antioxidant defense system of human body cannot neutralize the excessive levels of ROS produced by CPA. Antioxidant MOLE decreased oxidative stress that inhibited some CYPs, so inhibited rate of CPA metabolism and affecting CPA efficacy and toxicity. The elevated CPA levels increasing the risks; damage CYP structure leading to function loss or altered activity. MOLE also counteract harmful effects of CPA prevents oxidation of normal cells constituents; protect key cell components by neutralizing damage by the reactive short-lived ROS intermediates as natural byproducts of cell metabolism and produce by CYP. MOLE delay initiation or retard lipid oxidation reaction. The main physiological ROS source is the cellular respiration. The primary function of NADPH oxidases is to produce ROS. Free radicals disrupt living cells by oxidation of lipids, amino acids and carbohydrates as well as causing DNA mutations. Hormones mediators the stress reaction *in vivo* cortisol and catecholamine degenerate into particularly destructive free radicals.

Table 4 represented in-vitro cytotoxicity analysis of MOLE-CPA to human breast cancer cells lines. MO enhanced anticancer activities of CPA (kept cell viability of normal cells, increased toxicity of cancer cells and decreased IC_{50}) [39].

The values of IC_{50}, concentration of antitumor compound killed half of each tested cell lines were calculated from % cell viability-concentration plot [40], Table 4.

Table 5 showed the values of IC_{50} (μg/mL) of the free and MOLE combined CPA for MCF-7 cell lines.

USMOLE decreased IC_{50} from 198.88 μg/mL to 95.2 μg/mL for breast cancer cell lines.

The IC_{50} values of CPA and its combinations vary based on the tested specific cancer cell line, the other drugs in combination therapy and the experimental conditions. CPA combined with other agents, IC_{50} decrease, indicating enhanced efficacy and synergism. IC_{50} values for canine mammary tumor cell lines curcumin-CPA showed synergistic anti-proliferative effects towards CMT-U27 and CMT-U309 canine mammary cancer cells. Anti-proliferative activities of curcumin, CPA and a combination. Curcumin decreased the dose of CPA [41]. Much lower IC_{50} values obtained by CPA combination in treatment of ovarian cancer cell lines respond to CPA alone or combined heterogeneously depending upon histopathological features indicating individualized regimens may improve survival in ovarian cancer patients [42].

Table 3: Antioxidant activity (Decrease absorbance (%) DPPH

Sample	DPPH scavenging activity%	IC_{50}	DPPH reductase activity (IU)	% Inhibition
Ascorbic acid	87.91±0.001	30.1	0.003±0.03	98.62
CPA+ MOLE	73.24±0.008	33.21	0.0129±0.09	27.7

Table 4: The cell viability and toxicity of CPA against McF-7.

Cell line	MCR-5			MCF-7		
Conc. µg/mL	Mean O.D	S.E.	Viability %	Mean O.D	S.E.	Viability %
dilution	0.202	0.002	100	0.23	0.003	100.00
1500	0.030	0.004	14.827	0.023	0.001	10.00
750	0.073	0.005	36.079	0.048	0.002	20.87
375	0.158	0.003	77.924	0.086	0.002	37.246
187.5	0.197	0.002	97.529	0.103	0.006	44.928
93.75	0.200	0.002	99.012	0.194	0.003	84.203
46.87	0.195	0.002	96.540	0.228	0.002	99.275
23.43	0.202	0.002	99.671	0.237	0.005	103.188
11.71	0.199	0.006	98.517	0.227	0.004	98.841
IC_{50} (µg/mL)	814.423			181.504		

Table 5: Values of IC_{50} of MOLE and CPA to MCF-7 cell lines.

Compound	USMOLE	USMOLE-CPA	Heat MOLE	MCR-5
CPA-MO	218.45	95.2	615.2	814.423
CPA	181.504			

3.3. Toxicological effects of MOLE

While MOLE had high nutrition value with various health benefits. It's generally considered safe, there are some potential toxicological effects: excessive consumption MO lead to hyperthyroidism as phytochemicals stimulate thyroid gland. High doses associated with liver and kidney damage *in vivo* and more research needed to confirm these findings in humans. Individuals with allergies to plants in Moringaceae family experience allergy such as skin rashes, difficult breathing and swelling. MO interact with certain medications, especially for liver or thyroid gland. MOLE should be specified by healthcare professional before usage. Risks could be minimized by moderate dose, no excessive intake especially in underlying health conditions, with caution in case of pregnancy, breastfeeding or medications. Promising natural anti-inflammatory agent with potential therapeutic applications for a wide range of diseases [43].

4. Conclusion

The number and quality of bioactive chemicals from MOLE using US extraction were more advantageous than heat conventional extraction that required high purity selective solvent and involved degradation of some bioactive compounds because at operating temperature and long extraction duration and solvent evaporation. New non-conventional US extraction of MOLE validated. Extraction method (extraction time, temperature, solvent/sample ratio, water, number of extractions carried out), particle size. USMOLE was potent antioxidant Natural MOLE antioxidants can be used in modern medicine for scavenge reactive ROS species (free radicals in human body created during energy production, stress and medication by CPA. Antioxidants MOLE protect body against oxidative stress caused by increased ROS production and diminished levels of antioxidants. MOLE and enhanced antitumor activity of CPA by decreasing dose required (IC_{50}).

References

[1] Ahmed, J.H.; Makonnen, E.; Bisaso, R.K.; Mukonzo, J.K.; Fotoohi, A.; Aseffa, A.; Howe, R.; Hassan, M.; Aklillu, E. Population pharmacokinetic, pharmacogenetic, and pharmacodynamic analysis of cyclophosphamide in Ethiopian breast cancer patients. Frontiers in Pharmacology. 2020, 11, 1-14.

[2] Montoro, J.; Boumendil, A.; Finel, H.; Bramanti, S.; Castagna, L.; Blaise, D.; Dominietto, A.; Kulagin, A.; Yakoub-Agha, I.; Tbakhi, A.;Solano, C. Post-transplantation cyclophosphamide-based graft-versus-host disease prophylaxis in HLA-matched and haploidentical donor transplantation for patients with Hodgkin lymphoma: a comparative study of the

lymphoma working party of the european society for blood and marrow transplantation. Transplantation and Cellular Therapy. 2024. 30, 210-224.

[3] Balaha, M.F.; Alamer, A.A.; Aldossari, R.M.; Aodah, A.H.; Helal, A.I.; Kabel, A.M. Amentoflavone mitigates cyclophosphamide-induced pulmonary toxicity: involvement of-SIRT-1/Nrf2/Keap1 Axis, JAK-2/STAT-3 signaling, and apoptosis. Medicina. 2023, 59, 1-21.

[4] Pimenta, G.F.; Awata, W.M.; Orlandin, G.G.; Silva-Neto, J.A.; Assis, V.O.; da Costa, R.M. ; Bruder-Nascimento, T.; Tostes, R.C.; Tirapelli, C.R. Melatonin prevents overproduction of reactive oxygen species and vascular dysfunction induced by cyclophosphamide. Life Sci. 2024, 338, 1-12.

[5] Dixit, P.; Jeyaseelan, C.; Gupta, D. Nitrogen mustard: a promising class of anti-cancer chemotherapeutics–a review. Biointerface Research in Appl. Chem. 2022, 13, 135-161.

[6] Guidolin, V.; Jacobs, F.C.; MacMillan, M.L.;Villalta, P.W.; Balbo, S. Liquid Chromatography–Mass Spectrometry Screening of Cyclophosphamide DNA Damage *In Vitro* and in Patients Undergoing Chemotherapy Treatment. Chem. Research in Toxicology. 2023, 36, 1278-1289.

[7] Keshavarz-Bahaghighat, H.; Darwesh, A.M.; Sosnowski, D.K.; Seubert, J.M. Mitochondrial dysfunction and inflammaging in heart failure: novel roles of CPA derived epoxylipids. Cells. 2020, 9, 1-28.

[8] Krüger-Genge, A.; Köhler, S.; Laube, M.; Haileka, V.; Lemm, S.; Majchrzak, K.; Kammerer, S.; Schulz, C.; Storsberg, J.; Pietzsch, J.; Küpper, J.H. Anti-Cancer Prodrug Cyclophosphamide Exerts Thrombogenic Effects on Human Venous Endothelial Cells Independent of CYP450 Activation-Relevance to Thrombosis. Cells. 2023, 12, 1-20.

[9] Manavi, M.A.; Fathian Nasab, M.H.; Mohammad Jafari, R.; Dehpour, A.R. Mechanisms underlying dose-limiting toxicities of conventional chemotherapeutic agents. J. Chemotherapy. 2023, 1-31.

[10] Dixit, P.; Jeyaseelan, C.; Gupta, D. Nitrogen mustard: a promising class of anti-cancer chemotherapeutics–a review. Biointerface Research in Appl. Chem. 2022, 13, 135-161.

[11] Ayza, M.A.; Zewdie, K.A.; Tesfaye, B.A.; Wondafrash, D.Z.; Berhe, A.H. The Role of Antioxidants in Ameliorating Cyclophosphamide-Induced Cardiotoxicity. Oxidative Medicine and Cellular Longevity. 2020, 1, 1-14.

[12] Soliman, M.M.; Aldhahrani, A.; Alkhedaide, A.; Nassan, M.A.; Althobaiti, F.; Mohamed, W.A. The ameliorative impacts of Moringa oleifera leaf extract against oxidative stress and methotrexate-induced hepato-renal dysfunction. Biomedicine & Pharmacotherapy. 2020, 128, 1-10.

[13] Moichela, F.T.; Adefolaju, G.A.; Henkel, R.R.; Opuwari, C.S. Aqueous leaf extract of Moringa oleifera reduced intracellular ROS production, DNA fragmentation and acrosome reaction in Human spermatozoa *in vitro*. Andrologia. 2021, 53, 1-11.

[14] Hassan, M.A.; Xu, T.; Tian, Y.; Zhong, Y.; Ali, F.A.Z.; Yang, X.; Lu, B. Health benefits and phenolic compounds of Moringa oleifera leaves: A comprehensive review. Phytomedicine. 2021, 93, 1-16.

[15] Pareek, A.; Pant, M.; Gupta, M.M.; Kashania, P.; Ratan, Y.; Jain, V.; Pareek, A.; Chuturgoon, A.A. Moringa oleifera: An updated comprehensive review of its pharmacological activities, ethnomedicinal, phytopharmaceutical formulation, clinical, phytochemical, and toxicological aspects. Int. J. Molecular Sci. 2023, 24, 1-36.

[16] Faisal, M.A.; Octavianty, I.K.; Sujuti, H. ; Rudijanto, A. Anticataract Activity of Ethanolic Extract of Garcinia Mangostana Linn Pericarp on Glucose-induced Cataractogenesis in Goat Lens. Open Access Macedonian J. Medical Sci. 2020, 8, 571-577.

[17] Shady, N.H.; Mostafa, N.M.; Fayez, S.; Abdel-Rahman, I.M.; Maher, S.A.; Zayed, A.; Saber, E.A.; Khowdiary, M.M.; Elrehany, M.A.; Alzubaidi, M.A.; Altemani, F.H. Mechanistic wound healing and antioxidant potential of moringa oleifera seeds extract supported by metabolic profiling, in silico network design, molecular docking, and *in vivo* studies. Antioxidants. 2022, 11, 1-27.

[18] Singh, S.; Dubey, S.; Rana, N. Phytochemistry and pharmacological profile of drumstick tree "Moringa oleifera lam": an overview. Current Nutrition & Food Sci. 2023, 19, 529-548.

[19] Fetouh, H.A.; M Mailoud, O.; Hattawi, S.N.; Khamis, N.M.; S Alsubaie, M.; Alazmi, M. ; H Elsayed, A.; Abu ELazm, A.H.; H Alshammari, R. Synthesis, characterization and evaluation of optically active polar semi-organic glycine-cobalt chloride crystals. Alexandria Journal of Science and Technology. 2024, 126-134.

[20] Simon, S. K, S.; Joseph, J.; George, D. Optimization of extraction parameters of bioactive components from Moringa oleifera leaves using Taguchi method. Biomass Conversion and Biorefinery. 2023, 13, 11973-11982.

[21] El-Mossalamy, E.H.; Batouti, M.E.; Fetouh, H.A. The role of natural biological macromolecules: Deoxyribonucleic and ribonucleic acids in the formulation of new stable charge transfer complexes of thiophene Schiff bases for various life applications. Int. J. Biol. Macromol. 2021, 193, 1572-1586.

[22] Rajesh, Y.; Khan, N.M.; Shaikh, A.R.; Mane, V.S.; Daware, G.; Dabhade, G. Investigation of geranium oil extraction performance by using soxhlet extraction. Materials Today: Proceedings. 2023, 72, 2610-2617.

[23] Otu, P.N.Y.; Osae, R.; Abdullateef, M.T.; Cunshan, Z.; Xiaojie, Y.; Azumah, B.K., Characterization of Moringa oleifera leaf polysaccharides extracted by coupling ionic

liquid separation system with ultrasound irradiation. J. Food Process Eng. 2020, 43, 1-13.

[24] Fetouh, H.A. Facile route for processing natural polymers for the formulation of new low-cost hydrophobic protective hybrid coatings for carbon steel in petroleum industry. Polymer Bulletin. 2024, 1-20.

[25] Fetouh, H.A.; Ismail, A.M.; Hamid, H.A.; Bashier, M.O. Synthesis of promising nanocomposites from an antitumer and biologically active heterocyclic compound uploaded by clay and chitosan polymers. Int. J. Biol. Macromol. 2019, 137, 1211-1220.

[26] Rey-Stolle, F.; Dudzik, D.; Gonzalez-Riano, C.; Fernández-García, M., Alonso-Herranz, V., Rojo, D., Barbas, C.; García, A. Low and high resolution gas chromatography-mass spectrometry for untargeted metabolomics: A tutorial. Analytica Chimica Acta. 2022, 1210, 1-22.

[27] Okechukwu, V.U.; Eze, S.O.; Omokpariola, D.O.; Okereke, J.C. Evaluation of phytochemical constituents of Methanol extract of Moringa oleifera Lam. whole leaf by Gas Chromatography-Mass Spectrometry and Fourier transform infrared spectroscopy analysis. World News of Natural Sciences. 2021, 37, 18-30.

[28] Sallam, E. R.; S. F. Aboulnaga; A. M. Samy; D. M. Beltagy; J. M. El Desouky; H. Abdel-Hamid; H. A. Fetouh. Synthesis, characterization of new heterocyclic compound: pyrazolyl hydrazino quinoxaline derivative: 3-[5-(hydroxy1methyl)-1-phenylpyrazol-3-yl]-2-[2, 4, 5-trimethoxybenzylidine] hydrazonyl-quinoxaline of potent antimicrobial, antioxidant, antiviral, and antitumor activity. J. Molec. Structure. 2023, 1271, 1-10.

[29] Pinto, M.I.; Vale, C.; Sontag, G.; Noronha, J.P. Effects of ultrasonic irradiation and direct heating on extraction of priority pesticides from marine sediments. Int. J. Env. Analytical Chem. 2013, 93, 1638-1659.

[30] Fetouh, H.A.; Abd-Ellah, S.; Fadhil, F.M.; Ahmed, A.G.; Sallam, E.; Alazmi, M.; M Samy,A. ; Taha, A.; Hattawi, S.N.; El Desouky, J. Potential health risk effects of silver nanoparticles on aquatic ecosystem: Regulations and guidelines. Alexandria Journal of Science and Technology. 2024, 99-113.

[31] Fetouh, H.A.; Abdel-Hamid, H.; Zaghloul, A.A.H.; Ghadban, A.E.; Ismail, A.M. Formulation of promising antibacterial, anticancer, biocompatible and bioactive biomaterial as therapeutic drug delivery system for biologically active compound loaded on clay polymer. Polymer Bulletin. 2023, 80, 9989-10013.

[32] Pyka, A.L.I.N.A.; Babuska, M.; Zachariasz, M.A. A comparison of theoretical methods of calculation of partition coefficients for selected drugs. Acta Pol. Pharm. 2006, 63, 159-167.

[33] Szeto, H.H Cell-permeable, mitochondrial-targeted, peptide antioxidants. The AAPS J. 2006, 8, 277-283.

[34] Vongsak, B.; Sithisarn, P.; Gritsanapan, W. Simultaneous HPLC quantitative analysis of active compounds in leaves of Moringa oleifera Lam. J. Chromatographic Sci. 2014, 52, 641-645.

[35] Kim, H.J.; Chi, M.H.; Hong, I.K. Effect of ultrasound irradiation on solvent extraction process. J. Industrial and Eng. Chem. 2009, 15, 919-928.

[36] Okawa, H.; Saito, T.; Hosokawa, R.; Nakamura, T.; Kawamura, Y.; Sugawara, K. Effects of different ultrasound irradiation frequencies and water temperatures on extraction rate of bitumen from oil sand. Japanese J. Appl. Physics. 2010, 49, 7-12.

[37] Nagaoka, S.; Kuranaka, A.; Tsuboi, H.; Nagashima, U.; Mukai, K. Mechanism of antioxidant reaction of vitamin E: charge transfer and tunneling effect in proton-transfer reaction. J. Physical Chem. 1992, 96, 2754-2761.

[38] Bhattacharyya, S.; Sinha, K.; C Sil, P. Cytochrome P450s: mechanisms and biological implications in drug metabolism and its interaction with oxidative stress. Current Drug Metabolism. 2014, 15, 719-742.

[39] Anwar, F.; Latif, S.; Ashraf, M.; Gilani, A.H.Moringa oleifera: a food plant with multiple medicinal uses. Phytotherapy Research. 2007, 21, 17-25.

[40] Almufarij, R.S.; Ali, A.E.; Elbah, M.E.; Elmaghraby, N.S.; Khashaba, M.A., Abdel-Hamid, H.;Fetouh, H.A. Preparation, characterization of new antimicrobial antitumor hybrid semi-organic single crystals of proline amino acid doped by silver nanoparticles. Biomedicines. 2023, 11, 1-21.

[41] Alkan, F.U.; Anlas, C.; Cinar, S.; Yildirim, F.; Ustuner, O.; Bakirel, T.; Gurel, A. Effects of curcumin in combination with cyclophosphamide on canine mammary tumour cell lines. Veterinární Medicína. 2014, 59, 1-20.

[42] Ohta, I.; Gorai, I.; Miyamoto, Y.; Yang, J.; Zheng, J.H.; Kawata, N.; Hirahara, F.; Shirotake, S. Cyclophosphamide and 5-fluorouracil act synergistically in ovarian clear cell adenocarcinoma cells. Cancer Letters. 2001, 162, 39-48.

[43] Awodele, O.; Oreagba, I.A.; Odoma, S.; da Silva, J.A.T.; Osunkalu, V.O. Toxicological evaluation of the aqueous leaf extract of Moringa oleifera Lam.(Moringaceae). J. Ethnopharmacology. 2012, 139, 330-336.